Journal of Hazardous Materials 173 (2010) 427–432

Contents lists available at ScienceDirect

Journal of Hazardous Materials

journal homepage: www.elsevier.com/locate/jhazmat

Synthesis of nucleated glass-ceramics using oil shale fly ash

Jingde Luan, Aimin Li*, Tong Su, Xiaobo Cui

School of Environmental & Biological Science &Technology, Dalian University of Technology, Industrial Ecology and Environmental Engineering Key Laboratory of Ministry of Education, Dalian 116024, Liaoning, China

ARTICLE INFO

Article history:
Received 11 July 2009
Received in revised form 21 August 2009
Accepted 21 August 2009
Available online 27 August 2009

Keywords:
Glass-ceramics
Oil shale fly ash
Alkalinity
Crystalline phase

ABSTRACT

Nucleated glass-ceramics materials were produced from oil shale fly ash obtained from Huadian thermal power plant in China with the addition of analytic reagent CaO. On basis of differential thermal analysis (DTA) results, the nucleation and crystallization temperature of two parent glass samples with different alkalinity ($Ak = m_{CaO}/m_{SiO_2}$) were identified as $Tn_1 = 810\,^{\circ}C$, $Tc_1 = 956\,^{\circ}C$ and $Tn_2 = 824\,^{\circ}C$, $Tc_2 = 966\,^{\circ}C$, respectively. X-ray diffraction (XRD) analysis of the produced nucleated glass-ceramics materials revealed that there was a coexistence phenomenon of multi-crystalline phase and the main crystalline phase was anorthite ($[Ca,Na][Al,Si]_2Si_2O_8$). The microstructure of the glass-ceramics materials was examined by scanning electron microscope (SEM). SEM observation indicated that there was an increase in the quantity of sphere-shaped crystals when crystallization time increased. Furthermore, the increase of alkalinity caused more amorphous phase occurring in glass-ceramics materials. Through the tests of physical and mechanical properties, the glass-ceramics materials with more crystalline phase and fine microstructure had high density, fine performance of resisting compression (328.92 MPa) and negligible water absorption. Through chemical resistance tests, the glass-ceramics samples showed strong corrosion resistance. Overall results indicated that it was a feasible attempt to produce nucleated glass-ceramics materials for building and decorative materials from oil shale fly ash.

1. Introduction

As a possible energy source substitute, oil shale has been used to extract oil, generate electricity and supply heat [1]. Through fluidized-bed combustion of oil shale and semicoke, a great quantity of oil shale ash is generated. In China, the total annual discharge of oil shale ash considered as the by-product in utilization of oil shale, is estimated to be more than 800,000 tons. At the present time, oil shale ash is mainly disposed as landfill and partly used to produce construction materials such as cement and brick [2,3]. Therefore, it is important to develop new processing methods in order to implement widespread availability of these residues.

Previous studies show that oil shale ash is composed mainly of SiO_2, Al_2O_3, CaO and Fe_2O_3 with a variety of heavy metal oxides [1]. It is necessary to distinguish between fly ash and bottom ash because they have different chemical compositions [4]. The concentrations of heavy metals (e.g., Pb, Cd, Cr, Zn) in fly ash are higher than those in bottom ash. However, fly ash is directly used as the raw material for cement and brick production in China. Accompanying with recycling process of oil shale ash for construction materials, heavy metals are transferred into new products and may cause secondary pollution [5,6].

However, the primary oxides in oil shale fly ash (OSFA), such as SiO_2, Al_2O_3, CaO, makes OSFA suitable for the raw material to produce $CaO–Al_2O_3–SiO_2$ system glass-ceramics [7]. Vitrification by melting is proposed as a convenient method to solidify hazardous materials in which the glass product can immobilize and stabilize the heavy metals in the glass matrix [4,6]. It is possible that OSFA can be melted and transformed into chemical stable nucleated glass-ceramics material with low leachability of heavy metals [8]. Therefore, this kind of nucleated glass-ceramics material can be utilized widely in the building industry due to environmental-safe [9].

The present research concentrated on the production of nucleated glass-ceramics from OSFA obtained from a thermal power plant in northeast China. On basis of differential thermal analysis (DTA) results, the heat treatment of nucleated glass-ceramics production was identified. Furthermore, physical and mechanical properties (density, water absorption, pressive strength) and chemical resistance were examined in order to know whether the nucleated glass-ceramics produced from OSFA can be used as a construction material or a decoration material. These performance indexes of nucleated glass-ceramics are subjected to controlled crystallization, such as the content of crystalline phase, the form of tiny crystals, their number, growth rate and final size. These characteristics of crystalline phase in glass-ceramics are controlled by appropriated heat treatment [10]. Therefore, a discussion of the correlation between the heat treatment and the properties of nucle-

* Corresponding author. Tel.: +86 041184707448; fax: +86 041184707448.
E-mail address: leeam@dlut.edu.cn (A. Li).

0304-3894/$ – see front matter © 2009 Elsevier B.V. All rights reserved.
doi:10.1016/j.jhazmat.2009.08.099

Table 1
Chemical position of OSFA sample in experiment (wt%).

Component	OSFA	G1	G2
SiO_2	71.1307	60.9456	53.8325
Al_2O_3	12.0519	10.3262	9.1210
CaO	5.6811	19.1820	28.6107
Fe_2O_3	4.6071	3.9474	3.4867
SO_3	2.2621	1.9382	1.7120
K_2O	1.4713	1.2606	1.1135
MgO	1.2202	1.0455	0.9235
Ti_2O	0.5290	0.4533	0.4004
Na_2O	0.4093	0.3507	0.3098
MnO	0.2571	0.2203	0.1946
P_2O_5	0.2049	0.1756	0.1551
BaO	0.0598	0.0512	0.0453
SrO	0.0397	0.0340	0.0300
ZrO_2	0.0259	0.0222	0.0196
ZnO	0.0103	0.0088	0.0078
Rb_2O	0.0078	0.0067	0.0059

ated glass-ceramics was also presented in order to provide useful information for the optimization of technological parameters in glass-ceramics production from OSFA.

2. Experimental procedures

2.1. Experimental samples

OSFA used in this research was collected from the thermal power plant located in Huadian of Jinlin province, China. Through natural air drying and mechanical grading, fly ash with particle size <75 μm was selected to carry out experiment. The chemical composition of OSFA was determined by XRF (PDA-5500II, Shimadzu, Japan). It was clear that the main constitutes of OSFA were SiO_2, Al_2O_3, CaO. The chemical composition analysis indicated that OSFA was typical raw material for the most parent glass with ternary systems [11].

Two batches of experimental samples were prepared by mixing OSFA with analytic reagent CaO (Table 1). CaO additive was introduced in OSFA to increase the alkalinity of raw materials in order to lower the melting temperature and the melting viscosity. These raw materials were mixed together in agate pot by ball mill for 90 min.

2.2. Glass preparation

Well-mixed powder samples were melted in alumina crucible for 2 h in an electrically heated furnace at 1500 °C to ensure homogeneity of the melts. The melts were rapidly poured into water to form parent glasses.

2.3. Differential thermal analysis and heat treatment

Differential thermal analysis (DSC 404 F3, Netzsch, Germany) was used to investigate the thermal behavior of the parent glass samples, including the glass transition temperatures (*Tg*) and the crystallization peak temperatures (*Tc*). A less than 10 mg glass sample, crushed and ground to powder with particle size <75 μm, was put into a PtRh crucible with lid and then heated from room temperature to 1200 °C at the rate of 10 °C/min in static air. For further studies on microstructure and properties of produced glass-ceramics materials, the parent glass powder was filled in corundum crucible to obtain cylindrical samples with diameter 10 mm and height 3 mm and rectangular parallelepiped samples with 8 mm × 10 mm × 80 mm. Prepared samples were heat treated at the nucleation temperature (*Tn*) for 1.0 h, respectively. Being heated at the rate of 3 °C/min to *Tc*, experimental samples were crystallized at *Tc* for 1.0 h, 2.0 h, 3.0 h, 4.0 h, and then cooled naturally in the furnace.

2.4. X-ray diffraction studies and scanning electron microscope analysis

The crystalline phase and microstructure of the nucleated glass-ceramics materials were investigated by means of X-ray diffraction (XRD) and scanning electron microscope (SEM) techniques. Identification of crystalline phase of obtained nucleated glass-ceramics was performed by XRD (XRD-6000, Shimadzu, Japan). The glass-ceramics samples with diameter 10 mm and height 3 mm were prepared and analyzed over a range of 2θ angles from 10° to 90° using Cu Kα radiation at 40 KV and 30 mA settings. The resulting powder diffraction patterns were analyzed according to the Joint Committee on Powder Diffraction Standard data.

SEM (JSM-5600LV, JEOL, Japan) analysis was conducted on the nucleated glass-ceramics samples. Prepared samples were grounded flat by abrasive paper, polished with diamond paste to achieve a mirror-smooth surface, and then etched with HF solution (20 vol.%) for 90 s.

2.5. Properties tests

The physical properties of the nucleated glass-ceramics samples, including density, water absorption, were investigated by a series of experiments. The density and water absorption (%) of nucleated glass-ceramics samples were tested using the procedure outlined in GB/T 9966.3-2001. Pressive strength measurements were done on smooth surfaces of the glass-ceramics samples, using a universal test machine (CSS-2205, Changchun Testing Machine Institute, China). Referring to M.Erol's method and GB/T 9966.3-2001, the chemical resistances of nucleated glass-ceramics samples were tested in 10% H_2SO_4 and 10% NaOH solutions [11]. In this study, 1 g of prepared sample was treated at 373 K for 2 h in 50 ml solutions.

3. Results and discussion

3.1. Differential thermal analysis and optimum heat procedure

The glass transition temperature and crystallization temperature were determined by differential thermal analysis investigations on parent glass powder. From DTA curves of the two parent glass samples (Fig. 1), vitrification processes occurred around at Tg_1 = 760 °C and Tg_2 = 774 °C, respectively. Crystalliza-

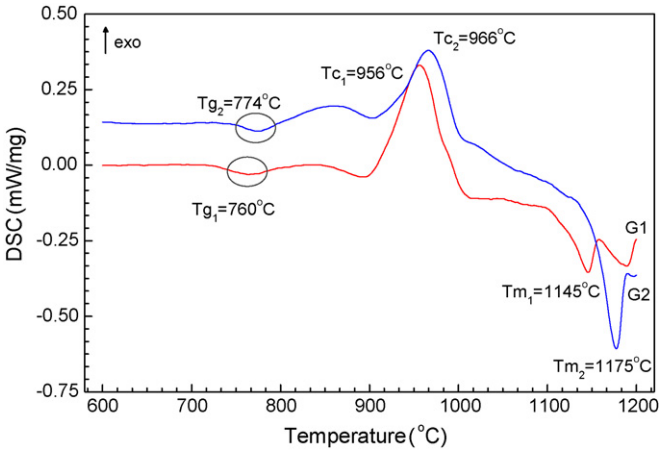

Fig. 1. DTA curve of parent glass powder G1 and G2.

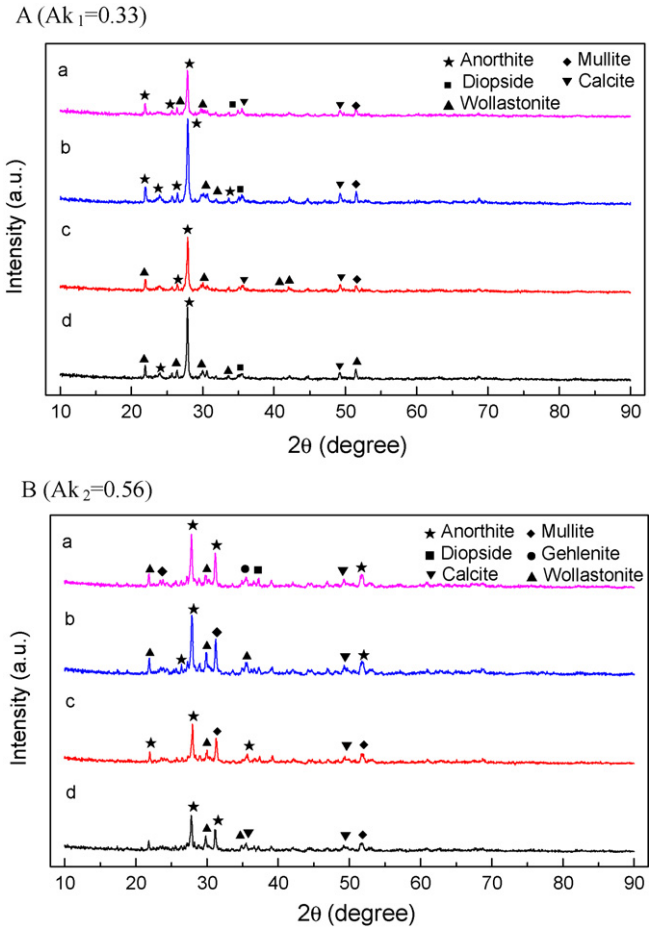

Fig. 2. XRD patterns of produced glass-ceramics samples with different crystallization time. (a—4.0 h, b—3.0 h, c—2.0 h, d—1.0 h).

tion temperatures of two parent glass samples were respectively identified as Tc_1 = 956 °C and Tc_2 = 966 °C. As the temperature rose, the melting temperatures of two glass samples appeared around at Tm_1 = 1145 °C and Tm_2 = 1177 °C, respectively. DTA results showed that the glass transition and crystallization temperatures of G1 sample were lower than those of G2 sample due to different amount of alkali metal oxides. In the glass samples, alkali metal oxides, including Fe_2O_3, K_2O, MgO, Ti_2O and Na_2O, led to lower energy input in crystalline phase transition.

The nucleation temperature was an important factor on nucleus formation. Previous studies showed that the optimum nucleation temperature usually occurred in the range from 50 °C to 100 °C above the glass transition temperature [12,13]. In our study, the nucleation temperatures of G1 and G2 samples were identified as Tn_1 = 810 °C and Tn_2 = 824 °C, respectively.

3.2. Microstructural characterization of producted glass-ceramics materials

XRD analysis was carried out to identify the crystalline phase on nucleated glass-ceramics materials. According to chemical analysis of two raw materials, $CaO–Al_2O_3–SiO_2$ (CAS) system glasses can be produced from industrial waste—OSFA. X-ray diffraction analysis revealed that the main crystalline phase was anorthite ($[Ca,Na][Al,Si]_2Si_2O_8$) in produced glass-ceramics materials (Fig. 2). Additionally, there were also wollastonite ($CaSiO_3$), diopside ($Ca[Mg,Al][Si,Al]_2O_6$), calcite ($[Ca,Mn]CO_3$), gehlenite ($Ca_2Al_2SiO_7$) and mullite ($Al_6Si_2O_{13}$) in glass-ceramics materials. Previous studies conformed that the crystalline phases such as anorthite, wollastonite, diopside, calcite, gehlenite and mullite were identified in the CAS type glass-ceramics from industrial wastes. The coexistence phenomenon of multi-crystalline phases indicated the complexity and uncertainty of nucleation and crystallization in the CAS glass system [11,14].

In Fig. 2, there were notable differences in the peak intensity of anorthite between G1 and G2 due to the different alkalinity ($Ak = m_{CaO}/m_{SiO_2}$). As the alkalinity increased from Ak_1 = 0.33 to Ak_2 = 0.56, the peak intensity decreased gradually. This phenomena indicated that the content of anorthite in G1 samples were higher than that in G2 samples. In Fig. 2A, there was the maximum of anorthite in glass-ceramics materials under the heat treatment of Tn_1 = 810 °C for 1.0 h and Tc_1 = 956 °C for 3.0 h.

According to the theory of stable energy of glass structure unit, the structure units of CAS system glass are $[SiO_4]$ and $[AlO_4]Ca[AlO_4]$ [15]. When heated at nucleation temperature, the free Ca^{2+} was prone to unite $[SiO_4]$ in order that wollastonite was first formed in glass-ceramics. During crystallization, the structure unit $[AlO_4]Ca[AlO_4]$ was forced to rearrange and unite $[SiO_4]$ to form anorthite as the main crystalline phase in CAS system glass-ceramics [12]. The metallic ions in parent glass were rearranged to give the structure of the crystals so that other crystalline phases like diopside, calcite, gehlenite and mullite can be formed in CAS system glasses-ceramics [11].

SEM investigations conduced to get a better understanding of the morphology of the microstructure [11]. SEM micrographs of glass-ceramics samples with different crystallization time are shown in Figs. 3 and 4. In Fig. 3, SEM observations revealed that a large number of sphere-shaped crystals occurred in the glass-ceramics materials. Under the heat treatment of Tn_1 = 810 °C for 1.0 h and Tc_1 = 956 °C for 1.0 h, the average crystal size of produced glass-ceramics sample was less than 350 nm (Fig. 3A). With the increase of crystallization time, the quantity of crystals in glass-ceramics was on the increase. Meanwhile, the sphere-shaped crystals became equirotal and aswarm. Under the heat treatment of Tn_1 = 810 °C for 1.0 h and Tc_1 = 956 °C for 4.0 h, the average crystal size of glass-ceramics sample was more than 1 μm (Fig. 3D). Previous studies indicated that the number and the size of the crystallites in glass-ceramics increased with the increase of crystallization time [11,16]. Moreover, the fine sphere-shaped crystals turned loosely cobble-shaped so that the better microstructure of glass-ceramics was broken. Although multi-crystalline phases in G2 samples were identified by XRD analysis, the amorphous phase appeared in vitrified material (Fig. 4) because the high amount of CaO made against the crystallization [17]. In Fig. 4, there were no obvious sphere-shaped crystals occurring in glass-ceramics materials. Therefore, the high alkalinity had an adverse effect upon the crystalline phases in glass-ceramics materials.

3.3. Physical and mechanical properties of glass-ceramics samples

Table 2 gives values for the pressive strength, density and water absorption of G1 and G2 samples. The pressive strength values of G1 samples were in the range of 233.44–328.92 MPa, which were higher than those of G2 samples. The difference in pressive strength indicated that the more crystalline phases in glass-ceramics materials conduced to enhance their pressive strength. In Table 2, the density values of G1 samples were in the range of 2.33–2.85 g/cm^3. Previous study indicated that the density of glass-ceramics samples increased with the enhancement of crystallization degree [11]. Therefore, the G1 sample produced under the heat treatment of Tn_1 = 810 °C for 1.0 h and Tc_1 = 956 °C for 3.0 h had the highest density value because of the highest crystallization degree in glass-ceramic samples. Due to lower crystallization degree, the density values of G2 samples were lower than those of G1 samples. In accompany with the increase of crystallization degree, the more

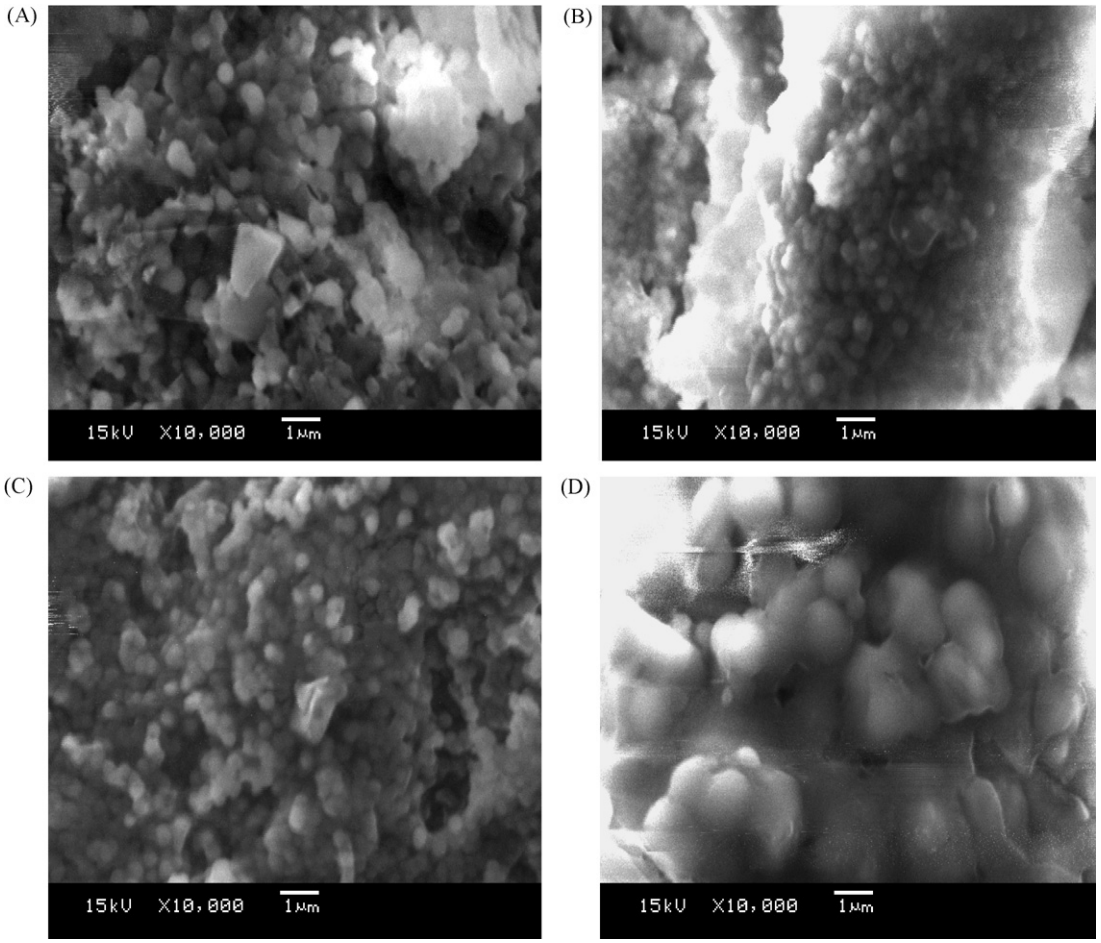

Fig. 3. SEM micrographs of G1 samples at different crystallization time. (A—1.0 h, B—2.0 h, C—3.0 h, D—4.0 h).

dense crystalline structure could be formed in order that the pore space between crystals gradually decreased. Therefore, there was an inverse relation between the water absorption and the density of glass-ceramics. By virtue of DTA analysis, the ratio *Tg*/*Tm* between glass transition and melting absolute temperature was calculated. Previous studies revealed that heterogeneous nucleation was dominate when $Tg/Tm > 0.58$. The crystallization mechanism was that the crystal growth started from the surface to the internal zone [18,19]. The high crystallization degree caused a reduction of the open porosity so that the glass-ceramics material showed good water resistance [20].

3.4. Chemical resistance of glass-ceramics materials

The chemical resistance of glass-ceramics samples was tested by immersion in H_2SO_4 and NaOH solutions. It can be seen that G1 samples showed better chemical stability than G2 samples (Table 3). Through the analysis of XRD and SEM, the increase of alkalinity in raw material caused more amorphous phase occurring in glass-ceramics. The durabilities of glass-ceramics samples correlated well with the crystallization degree of the produced samples [21]. Due to the lower crystallization degree, G2 samples became more unstable in stronger acid solution. Additionally, the durability of glass-ceramic samples also correlated with the morphological character of crystalline phase. The G1 glass-ceramic samples with fine microstructure showed higher resistance to strong acid solution. The difference in acid resistivity was also due to the higher amount of Al_2O_3 in glass-ceramics samples, which played the role of network former to strengthen the glass network [4]. Furthermore, the glass-ceramics samples in this study showed good stability in NaOH solution. According to the Ginsberg method, the proper mixture ratio of oxides in raw material predicted

Table 2
Properties of the glass-ceramics samples from OSFA.

Sample name	Heat treatment time (h)		Density (g/cm^3)	Water adsorption (wt.% loss)	Compression strength (MPa)
	Tn	*Tc*			
G1	1.0	1.0	2.69	0.56	233.44
	1.0	2.0	2.72	0.47	312.23
	1.0	3.0	2.85	0.42	328.92
	1.0	4.0	2.33	0.44	140.00
G2	1.0	1.0	2.27	1.31	135.29
	1.0	2.0	2.28	1.34	137.32
	1.0	3.0	2.35	1.03	159.11
	1.0	4.0	2.42	0.97	188.15

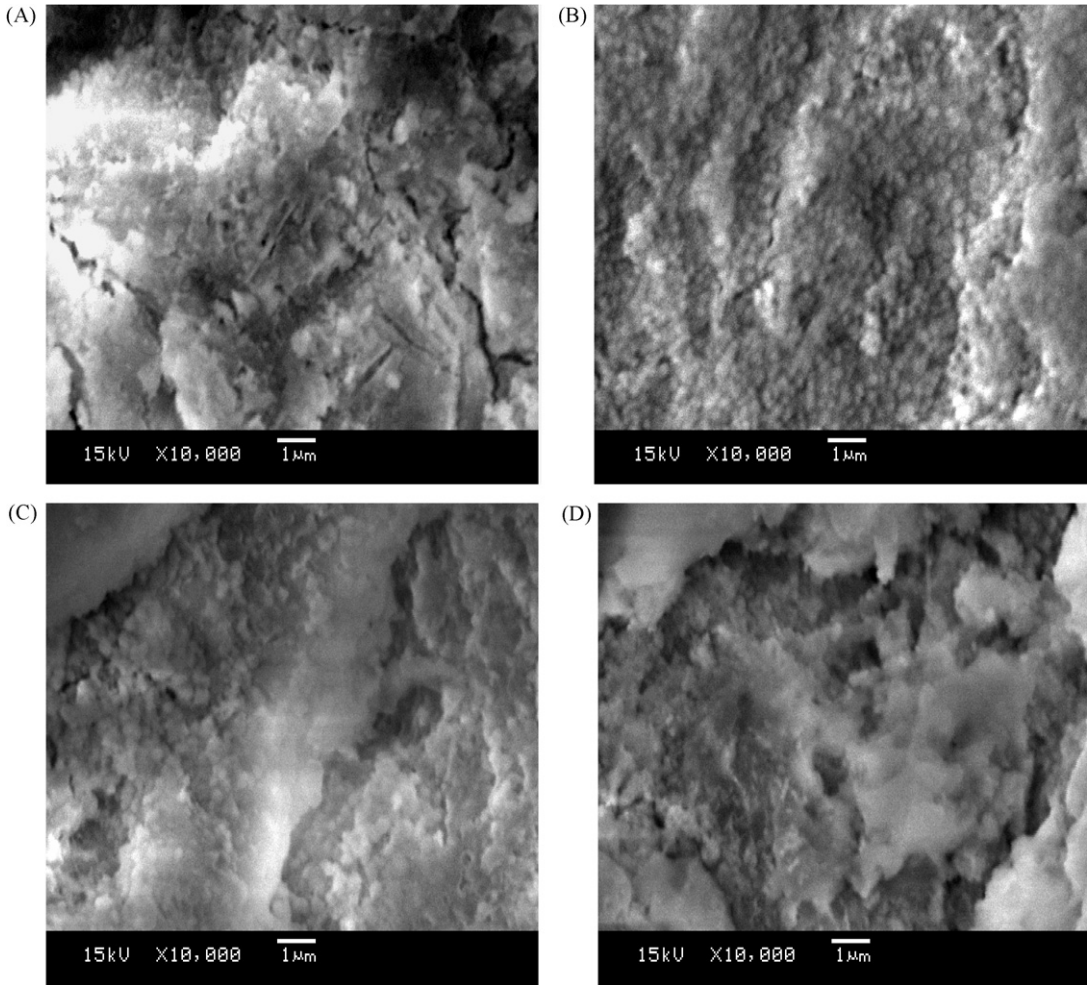

Fig. 4. SEM micrographs of G2 samples at different crystallization time. (A—1.0 h, B—2.0 h, C—3.0 h, D—4.0 h).

Table 3
Chemical resistances of the glass-ceramics samples from OSFA.

Sample name	Heat treatment time (h)		H_2SO_4 (wt.% loss)	NaOH (wt.% loss)
	Tn	*Tc*		
G1	1.0	1.0	1.45	Negligible
	1.0	2.0	1.23	Negligible
	1.0	3.0	0.97	Negligible
	1.0	4.0	1.63	Negligible
G2	1.0	1.0	2.90	Negligible
	1.0	2.0	2.45	Negligible
	1.0	3.0	2.60	Negligible
	1.0	4.0	2.83	Negligible

optimized glass-ceramics formation [18]. Moreover, the obtained glass-ceramics material had good chemical resistance, particularly in alkaline environment [4]. The investigations on chemical resistance revealed that the produced glass-ceramics from OSFA was a resistant material.

4. Conclusions

In this study, nucleated glass-ceramics materials were produced from OSFA with CaO additive. By DTA analysis, the nucleation and crystallization temperatures of two parent glass samples were identified as $Tn_1 = 810\,^{\circ}C$, $Tc_1 = 956\,^{\circ}C$ and $Tn_2 = 824\,^{\circ}C$, $Tc_2 = 966\,^{\circ}C$, respectively. XRD and SEM results revealed that there was a coexistence phenomenon of multi-crystalline phases in glass-ceramics materials and the main crystalline phase was anorthite ($[Ca,Na][Al,Si]_2Si_2O_8$). The increase of alkalinity caused more amorphous phase occurring in glass-ceramics. The glass-ceramics materials with fine sphere-shaped crystals were produced from raw material ($Ak_1 = 0.33$) under the heat treatment of $Tn_1 = 810\,^{\circ}C$ for 1.0 h and $Tc_1 = 956\,^{\circ}C$ for 3.0 h.

The glass-ceramics with fine microstructure showed better physical and mechanical properties and chemical resistance. The obtained glass-ceramics materials showed the maximum pressive strength of 328.92 MPa, lower water absorption and strong corrosion resistance. Therefore, it was a feasible attempt to produce nucleated glass-ceramics from OSFA.

Acknowledgement

This work was supported by the National High Technology Research and Development Program of China (863 Program) (Grant no. 2007.AA05Z333).

References

[1] X.M. Jiang, X.X. Han, Z.G. Cui, Progress and recent utilization trends in combustion of Chinese oil shale, Progress in Energy and Combustion Science 33 (6) (2007) 552–579.
[2] Xiang-peng Feng, Xue-lian Niu, Xue Bai, Xiao-ming Liu, Heng-hu Sun, Cementing properties of oil shale ash, Journal of China University of Mining and Technology 17 (4) (2007) 498–502.
[3] Awni Y. Al-Otoom, Utilization of oil shale in the production of portland clinker, Cement and Concrete Composites 28 (1) (2006) 3–11.
[4] L. Barbieri, A. Karamanov, A. Corradi, I. Lancellotti, M. Pelino, J. Ma Rincon, Structure, chemical durability and crystallization behavior of incinerator-based glassy systems, Journal of Non-Crystalline Solids 354 (2–9) (2008) 521–528.
[5] Jingde Luan, Aimin Li, Tong Su, Xuan Li, Translocation and toxicity assessment of heavy metals from circulated fluidized-bed combustion of oil shale in Huadian, China, Journal of Hazardous Materials 166 (6) (2009) 1109–1114.
[6] Jong Soo Park, Shoji Taniguchi, Young Jun Park, Alkali borosilicate glass by fly ash from a coal-fired power plant, Chemosphere 74 (2) (2009) 320–324.
[7] Suha Yuruyen, H. Ozkan Toplan, The sintering kinetics of porcelain bodies made from waste glass and fly ash, Ceramics International 35 (6) (2009) 2427–2433.
[8] F. Andreola, L. Barbieri, S. Hreglich, I. Lancellotti, L. Morselli, F. Passarini, I. Vassura, Reuse of incinerator bottom and fly ashes to obtain glassy materials, Journal of Hazardous Materials 153 (3) (2008) 1270–1274.
[9] Kuen-Sheng Wang, Kae-Long Lin, Ching-Hwa Lee, Melting of municipal solid waste incinerator fly ash by waste-derived thermite reaction, Journal of Hazardous Materials 162 (1) (2009) 338–343.
[10] A. Karamberi, A. Moutsatsou, Vitrification of lignite fly ash and metal slags for the production of glass and glass ceramics, China Particuology 4 (5) (2006) 250–253.
[11] M. Erol, S. Kucukbayrak, A. Ersoy-Mericboyu, Production of glass-ceramics obtained from industrial wastes by means of controlled nucleation and crystallization, Chemical Engineering Journal 132 (1–3) (2007) 335–343.
[12] Fei Peng, Kai-ming Liang, An-min Hu, Nano-crystal glass-ceramics obtained from high alumina coal fly ash, Fuel 84 (4) (2005) 341–346.
[13] A.R. Boccaccini, A.A. Francis, R.D. Rawlings, Production of glass-ceramics from coal ash and waste glass mixtures, Key Engineering Materials 206–213 (2002) 2049–2052.
[14] Fei Peng, Kaiming Liang, Anmin Hu, Hua Shao, Nano-crystal glass-ceramics obtained by crystallization of vitrified coal fly ash, Fuel 83 (14–15) (2004) 1973–1977.
[15] K.M. Liang, R.G. Duan, S.R. Gu, A study on the crystallizaton of $CaO–Al_2O_3–SiO_2$ system glasses, Journal of Materials Processing Technology 75 (1998) 235–239.
[16] M. Erol, S. Kucukbayrak, A. Ersoy-Mericboyu, The influence of the binder on the properties of sintered glass-ceramics produced from industrial wastes, Ceramics International 35 (7) (2009) 2609–2617.
[17] Young Jun Park, Soon Ok Moon, Jong Heo, Crystalline phase control of glass ceramics obtained from sewage sludge fly ash, Ceramics International 29 (2) (2003) 223–227.
[18] F. Andreola, L. Barbieri, A. Corradi, I. Lancellotti, R. Falcone, S. Hreglich, Glass-ceramics obtained by the recycling of end of life cathode ray tubes glasses, Waste Management 25 (2) (2005) 183–189.
[19] Young Jun Park, Jong Heo, Nucleation and crystallization kinetics of glass derived from incinerator fly ash waste, Ceramics International 28 (6) (2002) 669–673.
[20] L. Barbieri, A. Corradi, I. Lancellotti, T. Manfredini, Use of municipal incinerator bottom ash as sintering promoter in industrial ceramics, Waste Management 22 (8) (2002) 859–863.
[21] M. Erol, S. Kucukbayrak, A. Ersoy-Mericboyu, Comparison of the properties of glass, glass-ceramic and ceramic materials produced from coal fly ash, Journal of Hazardous Materials 153 (1–2) (2008) 418–425.